PENNSTATE

The High Energy Astrophysics ACIS Team

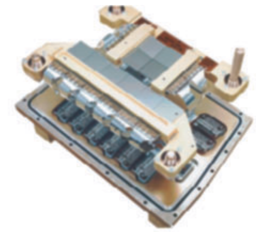

A Study of QSO Evolution in the X-ray Band with the Aid of Lensing: Discovery of a Possible Γ-Lx Relation

Xinyu Dai, George Chartas, Michael Eracleous & Gordon P. Garmire (Penn State Univ.)

Abstract

We present results from a mini-survey of relatively high redshift (1.7 < z < 4) gravitationally lensed radio-quiet quasars observed with the *Chandra X-ray Observatory* and with *XMM-Newton*. The lensing magnification effect allows us to search for changes in quasar properties such as the accretion process and the X-ray flux variability with redshift over three orders of magnitude in intrinsic X-ray luminosity. It extends the study of quasar properties to unlensed X-ray flux levels as low as a few times 1e-15 erg cm^{-2} s^{-1} in the observed 0.4-8 keV band. We present a spectral and temporal analysis of the X-ray properties of quasars at redshifts near the peak of their comoving number density, thought to have occurred at z~2.

We find a possible correlation between the X-ray photon index and X-ray luminosity of the gravitationally lensed quasar sample. The X-ray spectral slope steepens as the X-ray luminosity increases. This correlation is still significant when we combine the data from other samples of quasars with z > 1.5, especially in the low luminosity range between 1e43 - 3e45 erg/s. This result is surprising considering that such a correlation is not found for quasars with redshifts below 1.5.

The upper limits of X-ray variability scale of our relatively high redshift sample of lensed quasars are consistent with the known correlation between variability and luminosity observed in Seyfert 1s when this correlation is extrapolated to the larger luminosities of our sample.

We acknowledge the financial support by NASA grant NAS 8-01128.

Introduction

It is important to extend the study of quasars to high redshifts in order to understand the evolution of quasars and their environments. The X-ray band probes the innermost regions of the central engine of the Active Galactic Nuclei. The study of high-redshift quasars in X-rays may possibly answer the question of whether there is an evolution in the central engine and how it is related to the evolution of the quasar luminosity function.

The observed X-ray continuum emission of AGN is generally modeled by a power law. It is thought that this power-law component is produced by Compton scattering of soft photons on hot electrons in a corona. The study of this power-law component, its correlations with other AGN parameters, and its evolution reveals important information on the accretion process of the central object. The average photon index of this powerlaw component is ~1.9 in the 2-10 keV band. There is no strong evidence that the X-ray power-law index evolves with redshift or correlates with X-ray luminosity to date. Another important parameter which describes the broad band spectral shape of quasars is the optical-to-X-ray spectral index, α_{ox}, which is found to be dependent on the UV luminosity. In addition to spectral studies, variability studies of Seyfert galaxies show that the variability amplitude (excess variance) is anti-correlated with X-ray luminosity. Variability studies have been extended to quasars by several groups. The low redshift quasars (z < 2) are found to have an excess variance consistent with the variance-luminosity relation found in Seyfert 1s and there is a possible upturn of X-ray variability for high redshift quasars with z > 2.

Most of the observational and analysis techniques employed to date to study the faint high redshift quasars are based on either summing the individual spectra of many faint X-ray sources or obtaining deep X-ray observations of a few quasars. Although these techniques may yield important constraints on the average properties of high redshift quasars they each have significant limitations. Gravitational lensing provides an additional method for studying high redshift quasars. The extra flux magnification, from a few to ~100, provided by the lensing effect enables us to obtain high S/N spectra and light-curves of distant quasars with less observing time and allows us to search for changes in quasar properties, such as the accretion process and X-ray flux variability over three orders of magnitude in intrinsic X-ray luminosity.

Observations and Analysis

Table 1. The sample of Gravitational Lensed Radio-Quiet Quasars

Quasars	Redshift	BAL?	Galactic N_H[a] (10^{20} cm^{-2})	*Chandra* Exposure First[b] (ks)	*Chandra* Exposure Second[c] (ks)	*XMM-Newton* Exposure (ks)
HE 0230−2130	2.162	···	2.3	15	···	···
HS 0818+1227	3.115	···	3.4	20	···	···
APM 08279+5255	3.911	BAL	3.9	10	90	100
RX J0911.4+0551	2.80	mini-BAL	3.7	30	10	16
LBQS 1009−0252	2.74	···	3.8	10	···	···
HE 1104−1805	2.303	···	4.6	49	···	···
PG 1115+080	1.72	mini-BAL	3.5	26	10	60
Q 1208+101	3.80	···	1.7	10	···	···
H 1413+117	2.55	BAL	1.8	40	···	···
HE 2149−2745	2.033	BAL	2.3	10	···	···
Q 2237+0305	1.695	···	5.5	30	10	···

[a]The Galactic N_H is based on Dickey & Lockman (1990).

[b]The first *Chandra* exposure to the target.

[c]The second *Chandra* exposure to the target.

Most of the lensed quasars of our sample were observed with ACIS onboard *Chandra* as part of a GTO program (PI: G. Garmire). Three of the lensed quasars were also observed with XMM-*Newton.* Table 1 presents a log of observations, including redshifts, Galactic column densities, and exposure times. All of the sources observed with Chandra are located near the aim point of the ACIS-S array, which is on the back-illuminated S3 chip. The *Chandra* data were reduced with the CIAO 2.3 software tools provided by the *Chandra X-Ray Center*. The *XMM-Newton* data were analyzed with the standard analysis software, SAS 5.3.

Spectral Analysis:

A variety of models were fit to the specta of the lensed quasars employing the software tool XSPEC v11 (Arnaud 1996). For several sources containing absorption or emission lines we added Gaussian line components to model them. We obtained the photon indices, 0.2-2 and 2-10 keV rest frame lensed luminosities for the quasars in our sample from this analysis. Table 2 lists the spectral models used to fit the spectra and several results obtained from these fits. We also calculated the optical-to-X-ray spectral index, α_{ox}, from the optical and X-ray flux of the quasars. The α_{ox} values are also listed in Table 2.

Magnification Analysis:

Gravitational lensing produces a magnification of the observed flux. We searched in the literature for the magnification values. We also modelled this effect using the software tool gravlens 1.04 developed by C. Keeton. We assumed a singular isothermal elliptical (SIE) mass profile with external shear to model all the lenses in our sample. The estimated magnification factors are listed in Table 2. Table 2 also includes the unlesed X-ray luminosities of the quasars. We used H_0 = 50 km/s/Mpc and q_0 = 0.5 in order to be consistent with the cosmology assumed in previous studies.

Timing Analysis:

To estimate the relative variabilities of the light-curves of the lensed quasars of our sample we used the normalized excess variance (e.g., Nandra et al. 1997, Turner et al. 1999, Edelson et al. 2002) defined as :

$$\sigma^2_{rms} = \frac{1}{N\mu^2}\sum_{i=1}^{N}\left[(X_i-\mu)^2-\sigma_i^2\right]$$

N is the number of bins in the light-curve, X_i are the count-rates per bin, μ is the mean count-rate and σ_i are the errors of X_i. We constructed light-curves in 1000 s bins. This allowed sufficient counts in each bin for Gaussian statistics to be appropriate. The mean redshift of our sample is 2.62 and the mean bin size in the quasar restframe is about 270 s.This bin size is similar to that used in the timing analysis of the Seyfert 1 sample.

Table 2. Properties of the Gravitational Lensed Radio-quiet Quasars

Quasars	Redshift	Model[a]	Γ	M	L_x (0.2–2 keV) (erg s^{-1})	L_x (2–10 keV) (erg s^{-1})	α_{ox}	σ^2_{rms} (10^{-2})	$\chi^2_\nu(\nu)$	$P(\chi^2/\nu)$[c]
HE 0230-2130	2.162	pow	$1.93^{+0.08}_{-0.05}$	15	3.8×10^{44}	3.0×10^{44}	−1.35 ± 0.04	−0.5 ± 0.5	1.09(39)	0.33
HS 0818+1227	3.115	pow	$1.59^{+0.10}_{-0.08}$	10	2.9×10^{44}	4.4×10^{44}	−1.65 ± 0.05	−0.6 ± 2.0	0.90(22)	0.60
APM 08279+5255	3.911	absori*(pow+zgau+zgau)	$1.78^{+0.04}_{-0.04}$	142	2.4×10^{44}	2.6×10^{44}	−1.80 ± 0.01	−0.3 ± 0.2	0.86(235)	0.95
RX J0911+0551	2.8	zwabs*(pow+zgau)	$1.31^{+0.08}_{-0.10}$	17	5.3×10^{43}	1.5×10^{44}	−1.81 ± 0.04	−0.7 ± 2.3	0.99(26)	0.47
LBQS 1009-0252	2.74	pow	$1.9^{+0.2}_{-0.1}$	3.5	1.3×10^{45}	1.0×10^{45}	−1.56 ± 0.05	−3.1 ± 0.8	1.57(9)	0.12
HE 1104-1805	2.303	pow	$1.86^{+0.06}_{-0.04}$	12	3.6×10^{44}	3.3×10^{44}	−1.70 ± 0.03	1.1 ± 0.8	0.97(82)	0.55
PG 1115+080	1.72	absori*(pow+zgau+zgau)	$1.90^{+0.03}_{-0.03}$	26	3.1×10^{44}	2.5×10^{44}	−1.59 ± 0.01	−0.2 ± 0.3	1.15(200)	0.07
Q 1208+101	3.8	pow+zgau	$2.3^{+0.2}_{-0.2}$	3.1	4.6×10^{45}	2.2×10^{45}	−1.62 ± 0.06	−2.7 ± 0.9	1.13(6)	0.34
H 1413+117	2.55	zwabs*(pow+zgau)	$1.8^{+0.3}_{-0.3}$	23	1.7×10^{44}	2.0×10^{44}	−1.7 ± 0.1	−3.0 ± 2.5	0.86(19)	0.63
HE 2149-2745[d]	2.033	zwabs*pow	$1.4^{+0.6}_{-0.3}$	3.4	3.3×10^{43}	7.8×10^{43}	−2.1 ± 0.1	···	···	···
Q 2237+0305	1.695	zwabs*(pow+zgau)	$1.92^{+0.07}_{-0.06}$	16	4.0×10^{44}	3.7×10^{44}	−1.81 ± 0.02	−0.3 ± 0.1	1.13(153)	0.14

Spectra of the Lensed Quasars

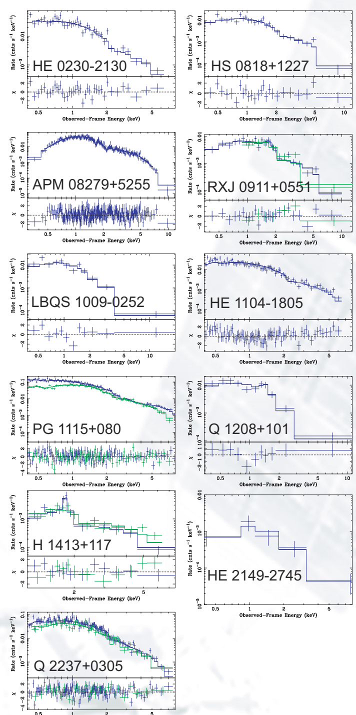

Light-curves of the Lensed Quasars

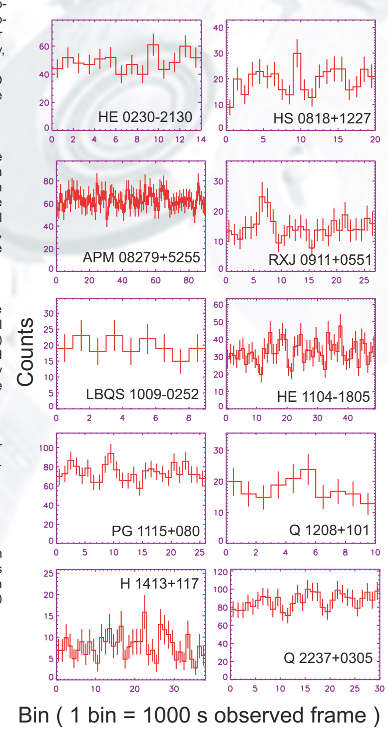

Results

1. Γ and Lx

Plots of (a) X-ray Luminosity vs. redshift. The squares represent 0.2--2 keV luminosities and crosses represent 2-10 keV luminosities. (b) X-ray photon index vs. redshift. (c) X-ray photon index vs. 0.2-2 keV luminosity. (d) X-ray photon index vs. 2-10 keV luminosity. We found a strong correlation between Γ and Lx in our lensed sample. The Spearman's rank correlation indicates a correlation significant at the 99.997% confidence level between Γ and 0.2-2 keV Lx. The correlation between Γ and 2-10 keV Lx is significant at the 98.6% confidence level. We did not find a correlation between Γ and redshift.

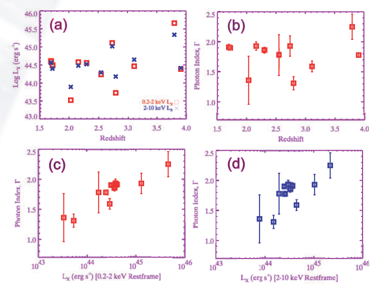

2. Different Γ-Lx Dependence between High-redshift and Low-redshift Quasars

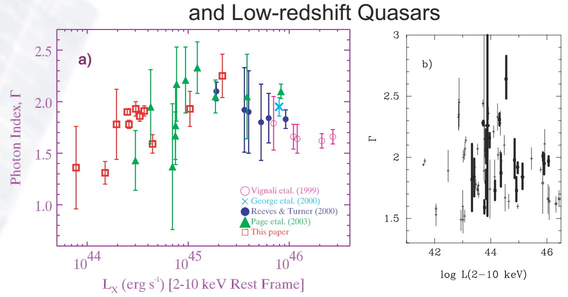

(a) Γ-Lx plot for quasars with z>1.5. The data shown as green filled triangles are from Page etal. (2003) The data shown as blue filled circles are from Reeves & Turner (2000) The data shown as cyan crosses are from George etal. (2000). The data shown as magenta open circles are from Vignali etal. (1999). The data shown as red open squares are from the present sample of lensed quasars. The high redshift quasars show strong dependence between Γ and Lx, especially in the low luminosity range where Lx < 3e45 erg/s. On the high luminosity end, the Γ dependence on Lx seems to flatten out or even has an anti-correlation pattern.

(b) Γ-Lx plot obtained from George etal. (2000). Most of data points are low-redshift (z<1.5) quasars and Seyfert 1s. There is no clear Γ-Lx dependence for the low-redshift quasars or Seyfert 1s. There are six z>1.5 quasars in this plot and these quasars are all included in plot (a).

3. α_{ox}

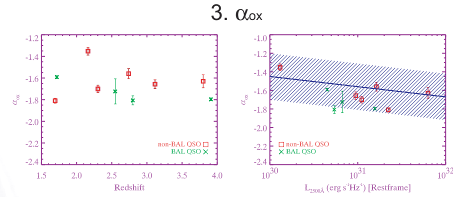

We did not find a strong correlation between α_{ox} on either redshift or on UV luminosity. However, most of our data points are consistent with the α_{ox}-L_{UV} correlation of Vignali etal. (2003).

4. Excess Variance

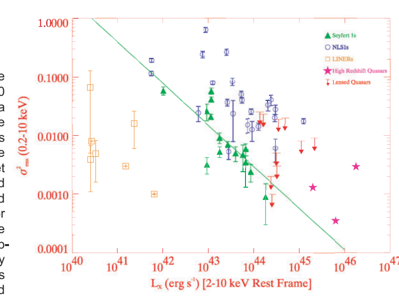

Excess variance in the 0.2-10 keV band vs. 2-10 keV luminosity. The data points representing the Seyfert 1s shown as green filled triangles were obtained from Nandra et al. (1997) and are fitted with a power law (solid line). The data points for the NLS1s shown as blue open circles were obtained from Leighly (1999). The data points for the LINERS and LLAGNs shown as orange squares were obtained from Ptak et al. (1998). The data points shown as magenta filled stars were obtained from z > 2 quasars of Manners et al. (2002). The downward arrows represent upper limits for the excess variances of the gravitationally lensed quasars from the present sample. Our upper limits are consistent with the known correlation observed in Seyfert 1s when extrapolated to larger luminosity.

References

Arnaud 1996, ASP Conf. Ser. 101: ADASS V, 5, 17d
Edelson et al. 2002, ApJ , 568,610
George et al. 2000, ApJ, 531,52
Leighly 1999, ApJ, 125, S317
Manners et al. 2002, MNRAS,330,390
Nandra et al. 1997, ApJ, 476, 70
Ptak et al. 1998, ApJ, 501, L37
Reeves & Turner 2000, MNRAS, 316, 234
Turner et al. 1999, ApJ, 524, 667
Vignali et al 1999, ApJ, 516, 582
Vignali et al. 2003, 125, 433